

## Effective forces between macroions: The cases of asymmetric macroions and added salt

E. Allahyarov,\* H. Löwen,<sup>†</sup> and S. Trigger\*

*Institut für Theoretische Physik II, Heinrich-Heine-Universität Düsseldorf, Universitätsstraße 1, D-40225 Düsseldorf, Germany*

(Received 6 June 1997; revised manuscript received 9 February 1998)

The distance-resolved effective forces between two spherical, highly charged colloidal macroions are calculated by computer simulation within the primitive model of strongly asymmetric electrolytes. In particular we consider the case of two asymmetric macroions, i.e., two particles with different charges and different radii, as well as the case of added salt ions. Different parameter sets corresponding to typical experimental samples are investigated. The results are compared with the predictions of traditional linear screening theory of Derjaguin and Landau [Acta Physicochim. URSS **14**, 633 (1941)] and of Verwey and Overbeek [*Theory of the Stability of Lyophobic Colloids* (Elsevier, Amsterdam, 1948)]. For moderate charge asymmetries we find a semiquantitative agreement and verify different scaling laws obtained from Derjaguin-Landau-Verwey-Overbeek (DLVO) theory justifying the DLVO description of binary mixtures and of charge- and size-polydisperse macroion samples. However for very large asymmetry, particularly for the mixture of charged and uncharged colloid particles, we obtain a nonzero repulsive interaction contrarily to DLVO theory. [S1063-651X(98)11805-6]

PACS number(s): 82.70.Dd, 61.20.Ja

### I. INTRODUCTION

The interactions between two highly charged colloidal particles (“macroions”) [1–3] in a polar solvent are frequently modeled by the traditional linear screening theory of Derjaguin, Landau, Verwey, and Overbeek [4,5]. Basically, this interaction consists of a pairwise screened Coulomb (or Yukawa) interparticle potential with a “renormalized charge” taking into account the finite core of the macroions. This Yukawa form was tested within theories that are beyond the linear screening level [6,7] and it was found that the interaction is indeed well described by a Yukawa potential, but the actual values of the screening length and the renormalized charge eventually have to be modified. Further indirect tests of the Derjaguin-Landau-Verwey-Overbeek (DLVO) picture have been done on different levels of numerical and theoretical sophistication (see, e.g., [8–13] and references therein). Except for a few cases, most of these tests were performed, however, for *salt-free* solutions of identical macroions being *monodisperse* in charge and radius. In fact, the case with symmetrical macroions and salt is much more frequently studied (see, e.g., [14–16,7]) than the case of asymmetric macroions where no such nonlinear screening theories have been considered as far as we are aware.

True experimental samples, however, are polydisperse in charge and size [17] and this has important consequences on the static structure factor for small wave vectors [18] and also shifts the freezing transition towards higher concentrations [19]. To deal with polydisperse systems theoretically, one frequently invokes the DLVO picture with a correspond-

ing size correction; see, e.g., [20]. Also, well-defined binary mixtures of low-charge and high-charge colloidal macroions can be prepared (see, e.g., [18,21]) and reveal many interesting effects not known from one-component systems. These binary mixtures were also described theoretically by DLVO theory [18,22–25].

The aim of the present paper is to check the validity of the DLVO picture for asymmetric macroions on the basis of “exact” computer simulation data of the “primitive” model of strongly asymmetric electrolytes involving all charged species including the macroions as well as the microscopic counterions and salt ions. Comparing the effective forces between two macroions confined in a box, we find that DLVO theory provides indeed a semiquantitative description of the interactions if the charge asymmetry is not too large. All the scaling laws inherent in DLVO theory are also in excellent agreement with our simulation data. Hence the use of DLVO theory is justified from a more microscopic background. At the same time, our results for the interaction between charged and uncharged colloids show the failure of DLVO theory. The latter predicts a zero interaction between such particles. However, as it will be shown below, the linear screening theory does not take properly into account the excluded volume of the neighboring particle, which leads to a nonzero value of the interaction.

We also performed computer simulations of the primitive model with added salt, which is relevant for any experiment. If the salt content is not too high, we again can justify the DLVO approach in this case. For large separations between the macroions, an effective attraction between the two macroions is also detected. However, it stems from the confining walls and is thus also relevant for strongly confined macroion pairs. The technique we are using has setup similar to that described in Ref. [26], where the case of symmetric macroions in salt-free solutions was studied.

Our paper is organized as follows. In Sec. II we give the definition of the effective force gained from statistical mechanics. We then briefly describe our simulation technique in

\*Permanent address: Institute for High Temperatures, Russian Academy of Sciences, Izorskaya Street 13/19, 127412 Moscow, Russia.

<sup>†</sup>Also at Institut für Festkörperforschung, Forschungszentrum Jülich, D-52425 Jülich, Germany.

Sec. III. The results are presented in Sec. IV. Section V is finally devoted to a discussion and an outlook.

## II. DEFINITION OF THE FORCES

The effective distance-resolved force between two macroions can be obtained from the effective potential [27,28]

$$U_{\text{eff}}(r) = U_1(r) + U_2(r), \quad (1)$$

where  $r$  is the distance between the macroion centres. The direct part  $U_1(r)$  of the interaction has the Coulomb form

$$U_1(r) = \frac{Z_1 Z_2}{\epsilon r} e^2, \quad (2)$$

where  $e$  is the elementary charge,  $Z_1$  and  $Z_2$  correspond to the macroion charge numbers, and  $\epsilon$  is the dielectric constant of the solvent ( $\epsilon = 81$  for water at room temperature). Without loss of generality we choose  $Z_1 > 0$  and  $Z_2 > 0$ . The indirect part  $U_2(r)$  in Eq. (1) can be written as

$$U_2(r) = -k_B T \ln(CZ_{CS}). \quad (3)$$

Here  $k_B T$  is the thermal energy,  $C$  is some irrelevant additive constant, and  $Z_{CS}$  is the canonical sum for the system of counterions plus salt ions,

$$Z_{CS} = \int \prod_{i=c,s} \prod_{k=1}^{N_i} d^3 r_k^{(i)} \exp\{-\beta(U_{cc} + U_{cm} + U_{ss} + U_{sm} + U_{cs})\}, \quad (4)$$

where

$$U_{ij} = \sum_{l=1}^{N_i} \sum_{k=1}^{N_j} V_{ij}(|\vec{r}_l^{(i)} - \vec{r}_k^{(j)}|),$$

$$U_{im} = \sum_{j=1}^{N_i} \sum_{l=1}^2 V_{im}^{(l)}(|\vec{r}_j^{(i)} - \vec{R}_l|), \quad (5)$$

with  $\beta = 1/k_B T$  being the inverse thermal energy. The pair potentials  $V_{ij}$  and  $V_{im}^{(l)}$  occurring in Eq. (5) are taken within the framework of the primitive model

$$V_{ij}(r) = \begin{cases} \frac{q_i q_j}{\epsilon r} e^2 & \text{for } r > \frac{\sigma_i + \sigma_j}{2} \\ \infty & \text{for } r < \frac{\sigma_i + \sigma_j}{2}, \end{cases} \quad (6)$$

$$V_{im}^{(l)}(r) = \begin{cases} \frac{q_i Z_m^{(l)}}{\epsilon r} e^2 & \text{for } r > \frac{\sigma_i + \sigma_m^{(l)}}{2} \\ \infty & \text{for } r < \frac{\sigma_i + \sigma_m^{(l)}}{2}, \end{cases}$$

where  $m$  denotes macroions,  $i$  and  $j$  denote the kind of species,  $i, j = c$  (counterions), and  $s$  (salt coions). In Eqs. (4) and (5)  $\vec{r}_k^{(i)}$  is the position of the small ion number  $k$  of species  $i$  with charge  $q_i$ .  $\vec{R}_1$  and  $\vec{R}_2$  are the positions of the two macroions. The parameters  $\sigma_i$  and  $\sigma_m^{(l)}$  are the diameters of the

core for small particles and macroions, respectively. For a fixed number of macroions  $N_m = 2$ , in general, we understand that  $Z_m^{(1)} \equiv Z_1$  and  $\sigma_m^{(1)} \equiv \sigma_1$  if the first macroion is considered and  $Z_m^{(2)} \equiv Z_2$  and  $\sigma_m^{(2)} \equiv \sigma_2$  if the second is considered. In Eq. (4)  $N_c$  is the total number of counterions (including also likely charged salt ions). Then the number of oppositely charged salt ions  $N_s$  is fixed by the global charge neutrality

$$|q_c|(N_c - N_s) = Z_1 + Z_2.$$

Here we assumed for simplicity that the salt ions have the same valence as the counterions.

One obtains the following form for the effective force  $\vec{F}_{\text{eff}}^{(1)}(r)$  [29] acting onto the first macroion:

$$\vec{F}_{\text{eff}}^{(1)}(r) = -\vec{\nabla}_{\vec{r}} U_1(r) - \vec{\nabla}_{\vec{r}} U_2(r), \quad (7)$$

with

$$-\vec{\nabla}_{\vec{r}} U_1(r) = \frac{Z_1 Z_2 e^2}{\epsilon r^3} \vec{r}. \quad (8)$$

From Eq. (6) we obtain two contributions to the indirect forces

$$-\vec{\nabla}_{\vec{r}} U_2(r) = \vec{F}_{\text{el}}^{(1)} + \vec{F}_{\text{cont}}^{(1)}, \quad (9)$$

where the electrical part is

$$\vec{F}_{\text{el}}^{(1)} = -\frac{Z_1 e^2}{\epsilon} \left\langle \sum_{i=c,s} \left( \sum_{j=1}^{N_i} \vec{\nabla}_{\vec{R}_1} \frac{q_i}{|\vec{r}_j^{(i)} - \vec{R}_1|} \right) \right\rangle \quad (10)$$

and the contact force  $\vec{F}_{\text{cont}}^{(1)}$  stemming from the excluded volume can be expressed as an integral over the surface of particle 1 of the contact equilibrium density of the microscopic ions,

$$\vec{F}_{\text{cont}}^{(1)} = -k_B T \oint d\vec{f} \sum_{i=c,s} \rho^{(i)}(\vec{r}), \quad (11)$$

where the surface vector  $\vec{f}$  points outside the sphere. Here

$$\rho^{(i)}(\vec{r}) = \left\langle \sum_{j=1}^{N_i} \delta(\vec{r} - \vec{r}_j^{(i)}) \right\rangle \quad (12)$$

and  $\vec{r} = \vec{R}_1 - \vec{R}_2$  is the separation distance between macroions. Furthermore, angular brackets denote a canonical average over the small ions. For an  $\{\vec{r}_j^{(i)}\}$ -dependent quantity  $A$ , the average is defined via

$$\langle A(\{\vec{r}_j^{(i)}\}) \rangle = \frac{1}{Z_{CS}} \int \prod_{i=c,s} \prod_{k=1}^{N_i} d^3 r_k^{(i)} \exp\{-\beta(U_{cc} + U_{cm} + U_{ss} + U_{sm} + U_{cs})\} A(\{\vec{r}_j^{(i)}\}).$$

The two terms (10) and (11) were discussed previously in the context of planar geometry [30–33].

In the absence of any system boundary, the force acting on second macroion  $\vec{F}_{\text{eff}}^{(2)}(r)$  has the same magnitude, but an opposite sign due to symmetry reasons, i.e.,  $\vec{F}_{\text{eff}}^{(1)}(r)$

$= -\vec{F}_{\text{eff}}^{(2)}(r)$ . Calculated values of  $\vec{F}_{\text{eff}}^{(1)}(r)$  can be compared with the predictions of DLVO theory where one has the expression

$$\vec{F}_{\text{DLVO}}(r) = \frac{Ze \exp\left(\frac{\sigma_1}{2R_D}\right)}{1 + \frac{\sigma_1}{2R_D}} \frac{Z_2 e \exp\left(\frac{\sigma_2}{2R_D}\right)}{1 + \frac{\sigma_2}{2R_D}} \frac{\exp\left(\frac{-r}{R_D}\right)}{\epsilon r} \times \left(\frac{1}{r} + \frac{1}{R_D}\right) \vec{r}. \quad (13)$$

The screening length  $R_D$  is given by

$$R_D^2 = \frac{\epsilon k_B T}{4\pi e^2 q_c^2 (n_c + n_s)}, \quad (14)$$

where  $n_i$  ( $i=c,s$ ) is the concentration of small ions  $n_i = N_i/V$ , with  $V$  the system volume.

### III. SIMULATION DETAILS

We consider a pair of charged macroions surrounded by a cloud of counterions and added salt ions. The system is confined in a cubic box of volume  $V$ , whose center is taken as the origin of our coordinate frame. The two macroions are placed symmetrically along the room diagonal of the cube such that the center of the cube coincides with the center of charge of the two particles:

$$r_1 = r \frac{Z_2}{Z_1 + Z_2}, \quad r_2 = r \frac{Z_1}{Z_1 + Z_2}. \quad (15)$$

Here  $r_i$  ( $i=1,2$ ) is the distance between the location of the macroion and the center of the box. The boundary conditions for small particles on the faces of the cube were chosen as a rigid wall, which imposes restrictions to the separation distance between macroions due to the wall effects. Therefore, to get results free from any artificial wall effects the following conditions are necessary: (a) the Debye spheres around the macroions should not penetrate the walls and (b) all the distances between macroions and walls must be larger than the separation distance  $r$ . We remark that, in general,  $\vec{F}_{\text{eff}}^{(1)}(r) \neq -\vec{F}_{\text{eff}}^{(2)}(r)$  due to the presence of the walls.

We performed a standard molecular-dynamics (MD) simulation [28]. The collision between small particles and the walls was modeled as reflection from the rigid surface. The value of the MD time step was adjusted in such a way that the displacement of the small particles was not greater than small percent of the macroion radius. The finite microscopic core of the oppositely charged small particles prevents them from collapsing into dipolar pairs.

Direct evaluation of Eq. (11), where the contact densities enter, is difficult since these densities pile up near the macroionic surfaces. However, the contact force  $\vec{F}_{\text{cont}}^{(1)}(r)$  can be obtained with a relatively small statistical error during the MD simulation by averaging the momentum transfer on the macroions during a collision with the microscopic ions.

### IV. SIMULATION RESULTS

The simulation parameters were chosen to be typical for charged colloidal suspensions:  $T=293$  K,  $\epsilon=81$ ,  $n_m=3.3 \times 10^{12} \text{ cm}^{-3}$ ,  $\sigma_1=1.11 \times 10^{-5} \text{ cm}$ , and the charge of the counterion and salt coion  $q_i = \pm 1$ . The diameter of the first macroion  $\sigma_1$  and the parameter  $F_0 = e^2/\sigma_1^2$  were used as the dimensionless measure for the distance and effective force. In these units, the length of the cubic cell determined as  $(L/\sigma_1)^3 = 2/n_m \sigma_1^3$  takes the value 7.64. We choose  $\sigma_c, \sigma_s = 10^{-3} \times \sigma_1$ .

The following sets A–M of parameters have been examined:

A:	$Z_1=280$ ,	$Z_2=280$ ,	$\sigma_2=\sigma_1$ ,	$n_s=0$ ;
B:	$Z_1=280$ ,	$Z_2=280$ ,	$\sigma_2=\sigma_1/2$ ,	$n_s=0$ ;
C:	$Z_1=310$ ,	$Z_2=250$ ,	$\sigma_2=\sigma_1$ ,	$n_s=0$ ;
D:	$Z_1=310$ ,	$Z_2=250$ ,	$\sigma_2=\sigma_1/2$ ,	$n_s=0$ ;
E:	$Z_1=360$ ,	$Z_2=200$ ,	$\sigma_2=\sigma_1$ ,	$n_s=0$ ;
F:	$Z_1=360$ ,	$Z_2=200$ ,	$\sigma_2=\sigma_1/2$ ,	$n_s=0$ ;
G:	$Z_1=410$ ,	$Z_2=150$ ,	$\sigma_2=\sigma_1$ ,	$n_s=0$ ;
K:	$Z_1=410$ ,	$Z_2=150$ ,	$\sigma_2=\sigma_1/2$ ,	$n_s=0$ ;
L:	$Z_1=560$ ,	$Z_2=0$ ,	$\sigma_2=\sigma_1$ ,	$n_s=0$ ;
M:	$Z_1=280$ ,	$Z_2=280$ ,	$\sigma_2=\sigma_1$ ,	$n_s=n_c/3$ ;
N:	$Z_1=280$ ,	$Z_2=280$ ,	$\sigma_2=\sigma_1$ ,	$n_s=n_c/2$ .

Run A was performed in [29] with a slightly different geometry for the macroions. Runs B–L take into account both the charge and size polydispersity for macroions. Runs A–L were done with  $N_c=560$  particles and run M was carried out for  $N_c+N_s=1120$  particles. Run N took the most simulation time and involved a total number of  $N_c+N_s=1680$  microscopic ions.

The equilibrium state of the system was checked during the simulation time for every run. This was done by a permanent monitoring of the temperature, average velocity, distribution function of velocities, and total potential energy of the system. On average it took from 2000 MD steps (for salt-free runs) to 10 000 MD steps (salt-added runs) to get the system into equilibrium. Then during 20 000–50 000 time steps we gather the statistics to perform canonical averages.

As it was mentioned in Sec. III, we are restricted to separation distances between macroions. For runs A–L the Debye sphere of macroions becomes comparable to the wall distance for a separation distance  $r \approx 3\sigma_1$ . For runs M and N this is the case for  $r \approx 5\sigma_1$  and  $6.5\sigma_1$ , respectively. For large distances spurious wall effects also contribute to the total force. In order to separate them from the effective macroion-macroion force we have performed reference runs with a single macroion in the box, surrounded only by its own counterions and salt ions. For parameter set A and particle 1, the resulting wall-induced force  $F_w = \vec{F}_w \cdot \vec{r}/r$  is shown in Fig. 1. Clearly, for symmetry reasons,  $F_w=0$  if the particle is centered in the cubic box ( $r=0$ ). The quantity  $F_w$  is negative, i.e., the wall-particle interaction is repulsive since the counterions gain Coulomb energy if the macroion is centered in the box. In the following we always subtract the wall forces from the total force. The result is an approximative

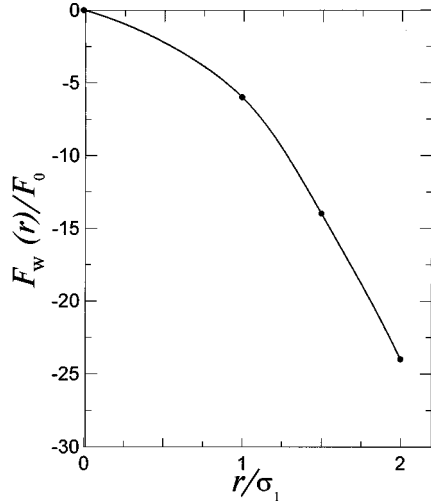


FIG. 1. Wall-induced force  $F_w(r)/F_0$  versus the reduced distance between the particle and the center of the cube,  $r/\sigma_1$ , for a one-particle simulation with charge  $Z=280$  in a cubic box. Hereinafter  $F_0=e^2/\sigma_1^2$ ,  $e$  is the elementary charge, and  $\sigma_1=1.11 \times 10^{-5}$  cm.

measure for the pure interparticle interaction. In all of our data the wall-induced forces are shown as vertical bars in the positive direction.

Our computer simulation results in the salt-free case for  $F_{\text{eff}}^{(1)}(r)=\vec{F}_{\text{eff}}^{(1)} \cdot \vec{r}/r$ , where  $r$  defines the macroion-macroion separation, are collected in Fig. 2. They are compared with DLVO theory predictions (solid line). It is easy to see from Fig. 2 that the points accounting for the calculated values of the effective forces are below DLVO theory. This implies that the DLVO potential *overestimates* the interactions. Still, as can be concluded from Fig. 2, DLVO theory provides a semiquantitative description of the simulation data.

A picture from run  $F$  is given in Fig. 3 for the separation distance  $r=2\sigma_1$ . A strong accumulation of counterions between the macroions can be seen, which implies a strong screening of the direct Coulomb interaction.

We have further checked whether the scaling rules predicted by DLVO theory are fulfilled by the calculated effective forces. For salt-free systems (runs A–K) we define the scaled force  $F^*(r)$  by

$$F^*(r) = \frac{F_{\text{eff}}^{(1)}(r)}{\frac{Z_1 \exp\left(\frac{\sigma_1}{2R_D}\right)}{1 + \frac{\sigma_1}{2R_D}} \frac{Z_2 \exp\left(\frac{\sigma_2}{2R_D}\right)}{1 + \frac{\sigma_2}{2R_D}}}. \quad (16)$$

Hence, in the framework of DLVO theory, the value of  $F^*(r)$  does not depend on the asymmetry of charges and sizes of macroions. The forces should fall on the same universal curve

$$F_{\text{DLVO}}^*(r) = \frac{e^{-r/R_D}}{\epsilon r} \left( \frac{1}{r} + \frac{1}{R_D} \right). \quad (17)$$

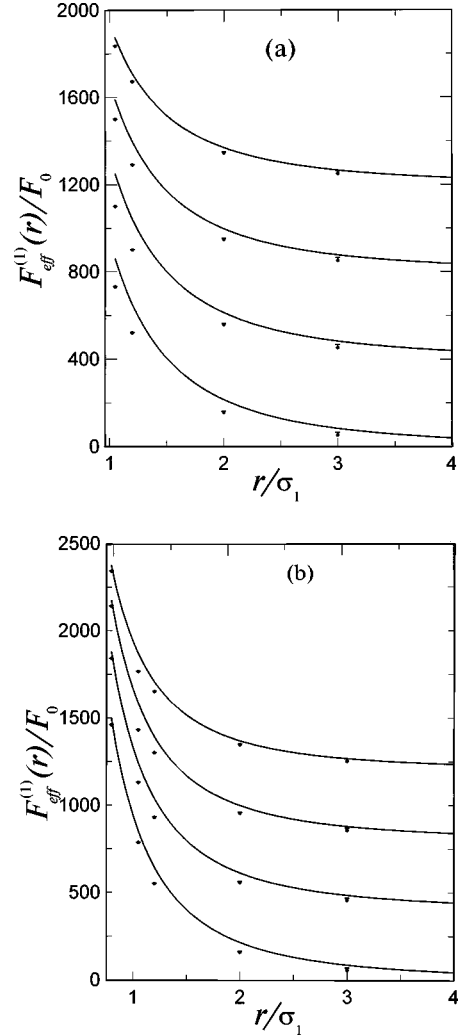


FIG. 2. Reduced effective force  $F_{\text{eff}}^{(1)}(r)/F_0$  versus the reduced macroion-macroion separation distance  $r/\sigma_1$  for, from bottom to top (a) runs A, C, E, and G and (b) runs B, D, F, and K. For the sake of clarity, the curves corresponding to runs C, E, and G in (a) and runs D, F, and K in (b) are shifted in the ordinates by 400, 800, and 1200 units accordingly. Dots represent computer simulation results. Vertical bars in the positive direction conform to the background induced forces (see the text). The solid line is the DLVO prediction  $F_{\text{DLVO}}(r)/F_0$ .

As it is clear from Fig. 4, the calculated values of the effective forces indeed obey this scaling rule except for very small  $r$ . (Note that for the chosen parameter combinations  $R_D$  does not change.) However, the actual form of the universal curve differs slightly from the DLVO expression (16). We have tried to fit our data for this universal curve with a Yukawa-type expression

$$F^*(r) \cong A^* \frac{e^{-r/R^*}}{\epsilon r} \left( \frac{1}{r} + \frac{1}{R^*} \right), \quad (18)$$

with two free fit parameters  $A^*$  and  $R^*$ . The best fit was obtained for  $A^*=0.85$  and  $R^*/R_D=0.7$ . It is included as a dashed line in Fig. 4. This demonstrates that the universal curve is indeed a Yukawa-type curve, but with parameters

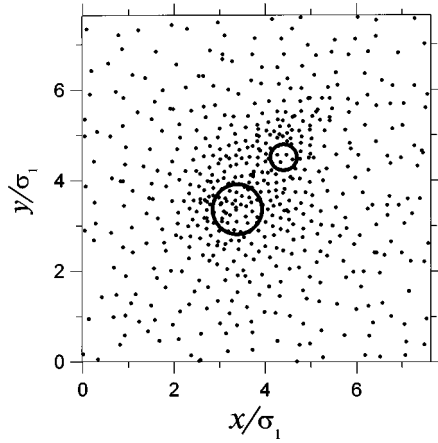


FIG. 3. Picture (projected to the  $xy$  plane) from run  $F$ . The separation distance  $r=2\sigma_1$ . The big open circles correspond to the core of macroions. The size of the counterions is magnified for visual convenience.

“renormalized” with respect to those arising from DLVO theory. This is consistent with earlier findings for symmetric macroions [6,7,11].

Drastical changes take place for run  $L$ , where one colloidal particle was neutral. According to Eq. (14), the charged particle is fixed at the center of the cubic box and the neutral particle was placed along the room diagonal of the cube. Therefore, wall-induced forces  $F_w$  on the particles vanish. As can be seen from Fig. 5, the interaction between particles is small but nonzero, contrary to the DLVO prediction. The charged particle is subjected to the electric force  $\vec{F}_{\text{el}}^{(1)}(r)$ , whereas the neutral one experiences only the contact force  $\vec{F}_{\text{cont}}^{(2)}(r)$ . Both forces are approximately equal, but have opposite direction, i.e.,  $\vec{F}_{\text{el}}^{(1)}(r) \approx -\vec{F}_{\text{cont}}^{(2)}(r)$ . Since the contact force is not included in the pure DLVO description, DLVO theory fails in predicting the force between a suspension of very-high-charge asymmetry. This repulsive force between charged and uncharged spheres may prevent them from coagulation. In previous theoretical studies such forces were neglected [34].

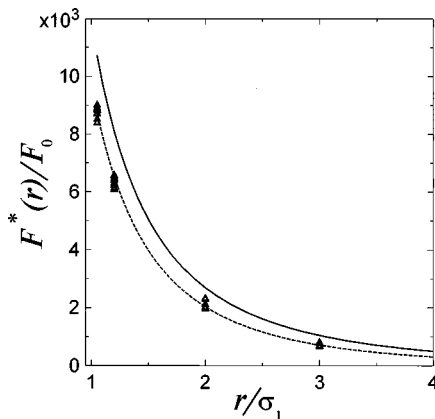


FIG. 4. Scaled force  $F^*(r)/F_0$  versus the reduced separation distance  $r/\sigma_1$ . Solid line, the DLVO prediction  $F_{\text{DLVO}}^*(r)/F_0$ ; open triangles, the simulation results in Fig. 2; dashed line, the best Yukawa fit as explained in the text.

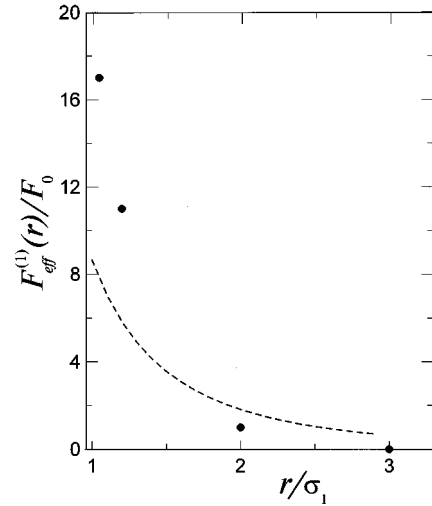


FIG. 5. Same as Fig. 2, but now for run  $L$ . The result for our approximative theory for the contact force is shown as a dashed line.

Let us finally discuss a simple analytical theory for the contact forces by extending the DLVO approach. In linear screening theory the counterion density field around the charged particle is approximately given by a Yukawa orbital

$$\rho^{(c)}(\vec{r}) \cong \frac{Z_1}{4\pi R_D^2} \frac{\exp\left(\frac{\sigma_1}{2R_D}\right) \exp\left(\frac{-|\vec{r}-\vec{R}_1|}{R_D}\right)}{1 + \frac{\sigma_1}{2R_D}}. \quad (19)$$

Inserting this into expression (11) and performing the surface integral leads to the following approximation for  $\vec{F}_{\text{cont}}(\vec{r})$ :

$$\vec{F}_{\text{cont}}(\vec{r}) \cong k_B T \frac{Z \exp\left(\frac{\sigma_1}{2R_D}\right)}{1 + \frac{\sigma_1}{2R_D}} \left[ \frac{\sigma_2}{2R_D} \cosh\left(\frac{\sigma_2}{2R_D}\right) - \sinh\left(\frac{\sigma_2}{2R_D}\right) \right] \exp\left(\frac{-r}{R_D}\right) \frac{r+R_D}{r^3} \vec{r}. \quad (20)$$

The corresponding results are also plotted in Fig. 5 as a dashed line. It can be seen that our theory describes the trends correctly, although it does not work well quantitatively. As expected from a comparison of the counterion density profiles [35], our theory underestimates the contact forces for small separations and correspondingly overestimates them for large separations.

In the simulations with added salt ions the screening length is reduced, which gives us the opportunity to investigate larger separations. In parallel, it is a good chance to check the screening length dependence of the DLVO poten-

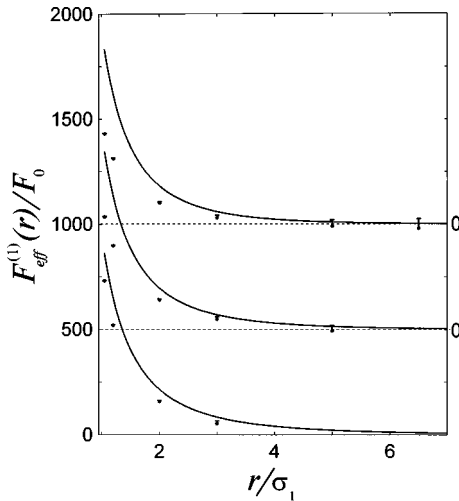


FIG. 6. Same as Fig. 2, but now for runs *A*, *M*, and *N* (from bottom to top).

tial. In Fig. 6 the effective forces are plotted for the case of added salt. Again DLVO theory overestimates the forces.

For runs *M* and *N* one can use another scaling function defined by

$$\Omega(R_D, r) = R_D$$

$$\times \ln \left( \frac{F_{\text{eff}}^{(1)}(r) \varepsilon r}{\frac{Z_1 \exp\left(\frac{\sigma_1}{2R_D}\right) Z_2 \exp\left(\frac{\sigma_2}{2R_D}\right)}{1 + \frac{\sigma_1}{2R_D} \quad 1 + \frac{\sigma_2}{2R_D}} \left(\frac{1}{r} + \frac{1}{R_D}\right)} \right) \quad (21)$$

in order to check the dependence of  $R_D$  on salt concentration. For the DLVO-predicted effective force this function turns out to be linear in  $r$ :  $\Omega(R_D, r) = -r$ . The calculated values for the scaled function  $\Omega(R_D, r)$  for runs *A*, *M*, and *N* are plotted in Fig. 7. The data indeed fall onto a straight line with slope  $-1$ , as predicted by DLVO theory. This proves that the dependence of  $R_D$  on the salt concentration is correctly described in DLVO theory. However, the line is shifted by a constant, which means that the actual charge prefactor is lower than that predicted by DLVO theory. This is again consistent with earlier findings [6,7,11].

## V. DISCUSSION AND OUTLOOK

To summarize, we have calculated, by ‘‘exact’’ computer simulation of the primitive model involving only two macroions, the effective forces between two macroions of different radius and different charge. For moderate charge asymmetries, we found that the traditional DLVO theory describes the data well semiquantitatively, though it overestimates the forces a bit, particularly for small macroion separations. The scaling laws for the size correction inherent in DLVO theory,

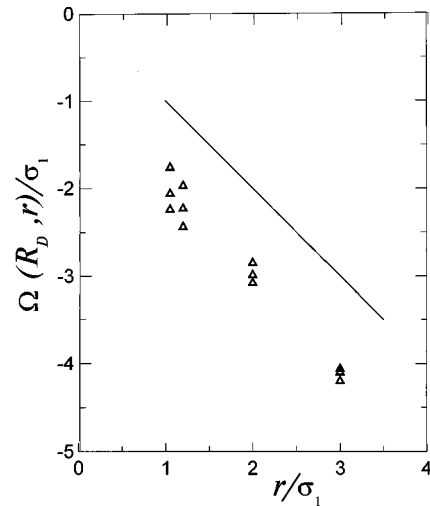


FIG. 7. Scaling function  $\Omega(R_D, r)/\sigma_1$  versus the reduced separation distance  $r/\sigma_1$ . Solid line, the DLVO prediction  $\Omega(R_D, r) = -r$ ; open triangles, the simulation results in Fig. 6.

which were used in many theoretical investigations [18,22–25], were also tested and found to be in excellent agreement with the simulation data. For large asymmetries, however, we show that there is a repulsive interaction between charged and uncharged colloidal particles, in disagreement with DLVO theory. We have also studied a pair of identical macroions with 1:1 salt added. In this case DLVO theory again works reasonably well and its scaling properties are consistent with our simulation data if the charge asymmetry is not too large.

We should point out, however, that our parameter combinations are limited. The concentration of added salt can be much higher and also the interaction between the macroions and counterion can be made stronger in real samples, e.g., by enhancing the bare macroion charge. A typical measure for the screening is the ratio of the macroion radius to the Debye radius  $\sigma_1/2R_D$ , which is between  $\frac{1}{6}$  (for the salt-free case) and  $\frac{1}{3}$  (for the salt-added case) for our data. Stronger deviations from the DLVO picture are expected when this ratio is of the order of 1 or larger [27]. If the screening becomes stronger we remark that the statistical error for the effective forces obtained from the computer simulation increases rapidly and it becomes impossible even to predict the correct sign of the force.

In future work we plan to investigate an ensemble of  $N_m = 3$  macroions where one can extract explicitly the role of triplet forces from the computer simulation data. Finally, we remark that a simulation of the primitive model with, say,  $N_m \approx 30$  highly charged macroions in a cube with periodic boundary conditions is highly desirable. However, such a simulation is still not possible on present-day computers due to the large number of counterions involved.

## ACKNOWLEDGMENT

This work was supported by the DFG within the SFB 237 (Unordnung und Grosse Fluktuationen).

- [1] For a review see K. S. Schmitz, *Macroions in Solution and Colloidal Suspension* (VCH, New York, 1993).
- [2] A. K. Sood, *Solid State Phys.* **45**, 1 (1991).
- [3] W. B. Russel, D. A. Saville, and W. R. Schowalter, *Colloidal Dispersions* (Cambridge University Press, Cambridge, 1989).
- [4] B. V. Derjaguin and L. D. Landau, *Acta Physicochim. URSS* **14**, 633 (1941).
- [5] E. J. W. Verwey and J. T. G. Overbeek, *Theory of the Stability of Lyophobic Colloids* (Elsevier, Amsterdam, 1948).
- [6] S. Alexander, P. M. Chaikin, P. Grant, G. J. Morales, P. Pincus, and D. Hone, *J. Chem. Phys.* **80**, 5776 (1984).
- [7] H. Löwen and G. Kramposthuber, *Europhys. Lett.* **23**, 673 (1993).
- [8] R. D. Groot, *J. Chem. Phys.* **95**, 9191 (1991).
- [9] H. Löwen, *Physica A* **235**, 129 (1997).
- [10] M. J. Stevens, M. L. Falk, and M. O. Robbins, *J. Chem. Phys.* **104**, 5209 (1996).
- [11] T. Gisler, S. F. Schulz, M. Borkovec, H. Sticher, P. Schurtenberger, B. D'Aguanno, and R. Klein, *J. Chem. Phys.* **101**, 9924 (1994).
- [12] F. Bitzer, T. Palberg, H. Löwen, R. Simon, and P. Leiderer, *Phys. Rev. E* **50**, 2821 (1994).
- [13] M. Fushiki, *J. Chem. Phys.* **97**, 6700 (1992).
- [14] C. W. Outhwaite and L. B. Bhuiyan, *Mol. Phys.* **74**, 367 (1991).
- [15] L. Degréve, M. Lozada-Cassou, E. Sánchez, and E. González-Tovar, *J. Chem. Phys.* **98**, 8905 (1993).
- [16] P. Attard, *J. Phys. Chem.* **99**, 14 174 (1995).
- [17] P. N. Pusey, in *Liquids, Freezing and the Glass Transition*, edited by J. P. Hansen, D. Levesque, and J. Zinn-Justin (North-Holland, Amsterdam, 1991).
- [18] R. Krause, B. D'Aguanno, J. M. Méndez-Alcaraz, G. Nägele, R. Klein, and R. Weber, *J. Phys.: Condens. Matter* **3**, 4459 (1991).
- [19] J. L. Barrat and J. P. Hansen, *J. Phys. (Paris)* **47**, 1547 (1986); P. G. Bolhuis and D. A. Kofke, *Phys. Rev. E* **54**, 634 (1996).
- [20] B. D'Aguanno and R. Klein, *Phys. Rev. A* **46**, 7652 (1992).
- [21] A. Meller and J. Stavans, *Phys. Rev. Lett.* **68**, 3646 (1992).
- [22] J. M. Méndez-Alcaraz, B. D'Aguanno, and R. Klein, *Physica A* **178**, 421 (1991).
- [23] E. Arrieta, C. Jedrzejek, and K. N. Marsh, *J. Chem. Phys.* **95**, 6806 (1991); **95**, 6838 (1991).
- [24] S. Sanyal and A. K. Sood, *Phys. Rev. E* **52**, 4154 (1995).
- [25] B. D'Aguanno, R. Krause, J. M. Mendez-Alcaraz, and R. Klein, *J. Phys.: Condens. Matter* **4**, 3077 (1992).
- [26] I. D'Amico and H. Löwen, *Physica A* **237**, 25 (1997).
- [27] H. Löwen, J. P. Hansen, and P. A. Madden, *J. Chem. Phys.* **98**, 3275 (1993).
- [28] See, e.g., M. P. Allen and D. J. Tildesley, *Computer Simulation of Liquids* (Clarendon, Oxford, 1989).
- [29] E. A. Allahyarov and S. A. Trigger (unpublished).
- [30] L. Guldbrand, B. Jönsson, H. Wennerström, and P. Linse, *J. Chem. Phys.* **80**, 2221 (1984).
- [31] R. J.-M. Pellenq, J. M. Caillol, and A. Delville, *J. Phys. Chem. B* **101**, 8584 (1997).
- [32] B.-Y. Ha and A. J. Liu, *Phys. Rev. Lett.* **79**, 1289 (1997).
- [33] J. P. Valleau, R. Ivkov, and G. M. Torrie, *J. Chem. Phys.* **95**, 520 (1991).
- [34] J. M. Méndez-Alcaraz, B. D'Aguanno, and R. Klein, *Langmuir* **8**, 2913 (1992).
- [35] H. Löwen and I. D'Amico, *J. Phys.: Condens. Matter* **9**, 8879 (1997).